# Performance Analysis of Noncoherent Digital Delay Locked Loops for Direct Sequence Spread Spectrum Systems With Doppler Shift and Quantized Adaptation

Wern-Ho Sheen, Ming-Jou Chang, and Cheng-Shong Wu

***Abstract*—The noncoherent second-order digital delay locked loop (DLL) with the presence of Doppler shift is investigated. The loop performance such as lock-in range, transient response, mean time-to-lose lock (MTLL), and mean square tracking error (MSE) are analyzed. The analysis is unique in two respects. First, MTLL and MSE are evaluated more accurately than by previous methods. Second, the impact of quantized adaptation on the loop performance is examined for digital DLL that was neglected previously. Numerical results show that: 1) the quantized adaptation may significantly alter the loop behaviors, including the lock-in range, transient responses, MTLL, and MSE; and 2) the traditional analysis based on Gaussian approximation may result in a large error in performance evaluation when quantized adaptation is taken into account.**

***Index Terms*—Direct sequence spread spectrum, doppler shift, noncoherent digital delay locked loops (DLLs), quantized adaptaion.**

## I. Introduction

PSEUDONOISE (PN) code synchronization is essential for direct-sequence spread spectrum (DSSS) systems to work effectively. PN code synchronization is achieved in two steps—code acquisition followed by code tracking [1], [2]. Code acquisition is a coarse alignment that aligns the received and local PN codes to a range that is suitable for code tracking. Code tracking, on the other hand, attempts to maintain fine synchronism of the two codes at all times. For global positioning systems (GPS's) and/or other broadcast applications, PN code synchronization follows a procedure of combined tracking/reacquisition/tracking, etc., after an initial acquisition. Both code acquisition and tracking have been active areas of research [1]–[18]. In this paper, we are only concerned with the code tracking part.

Manuscript received July 3, 2002; revised June 25, 2003; accepted September 19, 2003. The editor coordinating the review of this paper and approving it for publication is M. Sawahashi.

W.-H. Sheen is with the Department of Communication Engineering, National Chiao Tung University, Hsinchu 300, Taiwan, R.O.C. (e-mail: whsheen@cm.nctu.edu.tw).

M.-J. Chang is with the Computer and Communications Research Laboratories, ITRI, Hsinchu 310, Taiwan, R.O.C. (e-mail: mjchang@itri.org.tw).

C.-S. Wu is with the Department of Electrical Engineering, National Chung Cheng University, Chia Yi 621, Taiwan, R.O.C.

Digital Object Identifier 10.1109/TWC.2004.837662

Code tracking is mostly achieved with a delay locked loop (DLL). Extensive research has been devoted to the design, analysis, and implementation of DLLs. For example, different types of multipath resistant DLLs were proposed in [3]–[6] for the multipath environment, effective DLLs were proposed for GPS code tracking in [7]–[9], and efficient implementation was discussed in [10] for different types of DLLs. As to the performance analysis, the first-order analog DLL was analyzed thoroughly in [11], [12] for the additive white Gaussian noise (AWGN) channel. Specifically, in [12], mean square error (MSE) and mean time-to-lose lock (MTLL) are obtained by applying the renewal theory approach. This approach was extended in [13] to include the effects of multipath fading and multiuser access interference. The second-order analog DLL was analyzed in [16], where approximate MSE and MTLL were obtained for high signal-to-noise ratios (SNRs), under the presence of Doppler shift. On the other hand, digital DLLs were analyzed in [14]–[17]. In particular, in [14], MSE and MTLL of the first-order loop were evaluated for a band-limited system, and in [15] emphasis was on the effect of carrier frequency uncertainty on the MSE performance. In [17], MSE of the first- and second-order loops were obtained particularly for the GPS applications, and finally in [18], MSE is obtained for a low-complexity DLL with 1-b noncommensurate sampling. Digital code tracking becomes very popular because of the evolution toward all digital modem implementation of DSSS systems.

In this paper, accurate nonlinear analysis for the noncoherent second-order digital code tracking loops is investigated over AWGN channels with the presence of Doppler shift. This modeling of channel finds applications in GPS [17] and other civilian or military satellite-based DSSS systems, where Doppler shift is due to the relative movement between the satellite and the receiver. In the analysis, based on a regenerative Markov chain modeling of the code tracking process, the lock-in range, transient response, MSE, and MTLL are evaluated more accurately than the traditional analysis. Furthermore, in a digital DLL, the adaptation of code tracking can only be done in discrete steps, i.e., quantized adaptation and that will result in significant changes in the loop performance. In this analysis, the effect of quantized adaptation is evaluated as well.

The rest of this paper is organized as follows. Section II describes the noncoherent second-order digital DLL. In Sec-

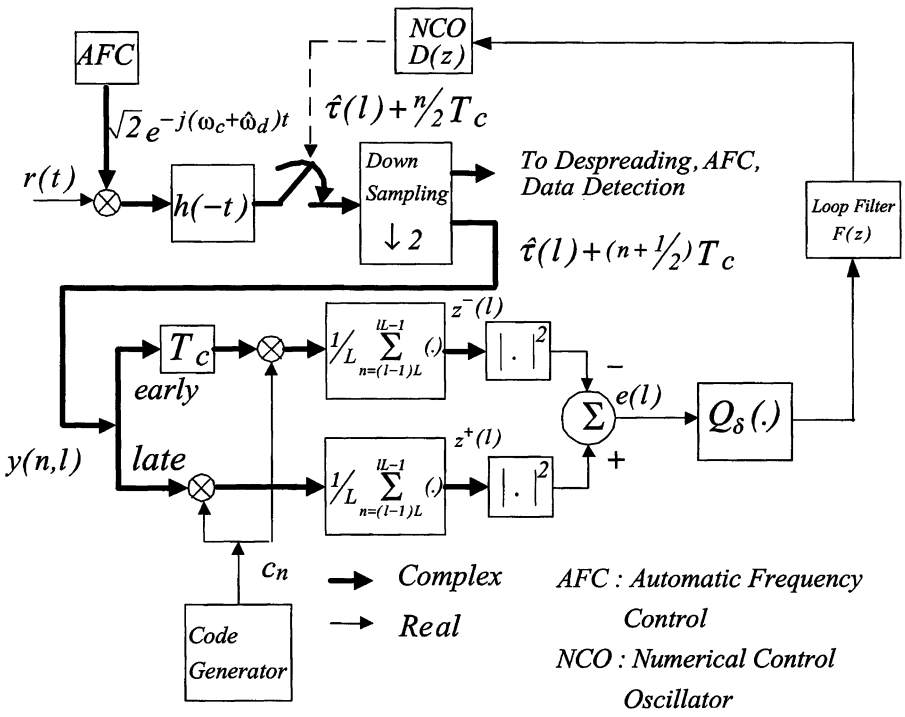


Fig. 1. Noncoherent digital DLL.

tion III, an accurate nonlinear analyzes is given to obtain the lock-in range, transient response, MSE, and MTLL, with emphasis on the effects of code Doppler and quantized adaptation. In Section IV, some numerical results are given and discussed. Finally, conclusions are given in Section V.

## II. Noncoherent DLL

A typical digital code tracking system for DS spread spectrum signals is shown in Fig. 1. After frequency translation, chip matched filtering, and down sampling, the code phase of the received signal is tracked by a noncoherent digital DLL. In Fig. 1, $\hat{w}_d$ is the estimated carrier shift obtained in the code acquisition stage. The sampling could also be done in front of chip matched filter. In any case, at least two times of over-sampling is needed for proper operation of DLL. In this study, the two-times over-sampling is employed. After down-sampling, as shown in Fig. 1, the sampled signal is directed to two different routes. The integer–chip samples are directed to a despreading unit for the subsequent carrier recovery, data detection and other signal processing, and the half-chip samples (early and late samples) are directed to a digital DLL for fine code tracking.

The correlation in the early or late branches of the digital DLL can be of passive types (moving average) or active (integrate and dump). For passive correlation, the code phase estimate is adjusted once per chip time $T_c$ and, hence, the digital DLL can track $L$ times code Doppler than by using active correlation, where the code phase estimate is adjusted once per $LT_c$. $L$ is the number of chips involved in the correlation. Nevertheless, passive correlation has a complexity of $L$ times larger than that of active correlation. Since there is no difference between these two types of correlations from the performance analysis point of view, only active correlation will be considered in this paper.

Let the received signal be denoted as $r(t)$. Then, for an AWGN channel with the presence of Doppler shift, we have

$$r(t)=\sqrt{2E_c}\sum_{m=-\infty}^{\infty}c_m h\left(t-mT_c-\tau(t)\right)\times\cos\left[(w_c+w_d)t+\theta\right]+n(t) \quad (1)$$

where $E_c$ is the chip energy, $c_m$ is the spreading sequence, and $h(t)$ is a shaping function with

$$\int_{-\infty}^{\infty}h^2(t)dt=1 \quad (2)$$

where $\tau(t)$ and $w_d$ are the time-varying code-phase shift and carrier-frequency shift due to Doppler effect, respectively. In addition, $\theta$ is the initial phase uncertainty, and $n(t)$ is AWGN with two-sided power spectral density $N_0/2$ watts/hertz. In this paper, instead of considering a specific system, we do the analysis over an AWGN channel with the presence of Doppler shift. As mentioned, the channel model finds application in GPS and other satellite-based DSSS systems.

Without considering the acceleration which is small in practice, the time-varying code-phase shift $\tau(t)$ is obtained as $\tau(t)=s(t)/c+t_0$, where $s(t)=v\cdot t$ is the time-varying distance between the satellite and receiver, $t_0$ is the initial delay at $t=0$, and $v$ and $c$ are the speed of the satellite and light, respectively. Define $a=v/c$, $\tau(t)=at+\tau_0$. In practice, $a\ll 10^{-4}$ and is called as the normalized code Doppler factor [19].

Let $y_c(t)$ and $y_s(t)$ be the in- and quadrature-phase components at the matched filter output. Then

$$y_c(t) = \sqrt{E_c} \sum_{m=-\infty}^{\infty} c_m \left[h(t - mT_c - at - \tau_0) \otimes h(t)\right] \times \cos(w_\Delta t + \theta) + \eta_c(t) \quad (3)$$

and

$$y_s(t) = \sqrt{E_c} \sum_{m=-\infty}^{\infty} c_m \left[h(t - mT_c - at - \tau_0) \otimes h(t)\right] \times \sin(w_\Delta t + \theta) + \eta_s(t) \quad (4)$$

where $w_\Delta = w_d - \hat{w}_d$, $\otimes$ denotes convolution, and $\eta_c(t)$ and $\eta_s(t)$ are the baseband in- and quadrature-phase white Gaussian noise, respectively. After sampling at $\hat{\tau}(l) + (n+1/2)T_c$, it can be shown that for the case $a \ll 1$, the half-chip samples are give by

$$y_c(n,l) = \sqrt{E_c} \sum_{m=-\infty}^{\infty} c_m R_h \times \left[\left(\hat{\tau}(l) + \left(n + \frac{1}{2}\right)T_c\right) - mT_c - \tau_0\right] \times \cos(w_\Delta n T_c + \theta_l) + \eta_c\left(n + \frac{1}{2}, l\right) \quad (5)$$

and

$$y_s(n,l) = \sqrt{E_c} \sum_{m=-\infty}^{\infty} c_m R_h \times \left[\left(\hat{\tau}(l) + \left(n + \frac{1}{2}\right)T_c\right) - mT_c - \tau_0\right] \times \sin(w_\Delta n T_c + \theta_l) + \eta_s\left(n + \frac{1}{2}, l\right) \quad (6)$$

where $\hat{\tau}(l)$ is the code phase estimated at the instant of $l \cdot LT_c$, $n$ is the chip index, $\theta_l = w_\Delta(T_c/2 + \hat{\tau}(l)) + \theta$, $\eta_c(n+1/2, l)$ and $\eta_s(n+1/2, l)$ are independent Gaussian noises with variance equal to $N_0/2$, and

$$R_h(\xi) = \int_{-\infty}^{\infty} h(\zeta)h(\zeta - \xi)d\zeta \quad (7)$$

is the auto-correlation function of the chip-matched filter.

Furthermore, after correlation, the complex-valued early and late correlator outputs are defined as

$$\boldsymbol{z}^{\pm}(l) \doteq z_c^{\pm}(l) + \boldsymbol{j} z_s^{\pm}(l). \quad (8)$$

Writing $z_c^{\pm}(l)$ and $z_s^{\pm}(l)$ as the sum of their DC and noise terms, we have, for the case of $a \ll 1$

$$z_c^{\pm}(l) = \mathrm{E}\left[z_c^{\pm}(l)\right] + N_c^{\pm}(l) \quad (9)$$

and

$$z_s^{\pm}(l) = \mathrm{E}\left[z_s^{\pm}(l)\right] + N_s^{\pm}(l) \quad (10)$$

where

$$\mathrm{E}\left[z_c^{\pm}(l)\right] \approx \frac{\sqrt{E_c}}{L} \sum_{n=(l-1)L}^{lL-1} R_h\left(\hat{\tau}(l) - \tau(n) \pm \frac{T_c}{2}\right) \times \cos(w_\Delta n T_c + \theta_l) \quad (11)$$

$$\mathrm{E}\left[z_s^{\pm}(l)\right] \approx \frac{\sqrt{E_c}}{L} \sum_{n=(l-1)L}^{lL-1} R_h\left(\hat{\tau}(l) - \tau(n) \pm \frac{T_c}{2}\right) \times \sin(w_\Delta n T_c + \theta_l) \quad (12)$$

$\tau(n) \doteq \tau(nT_c)$

$$N_c^{\pm}(l) = \frac{\sqrt{E_c}}{L} \sum_{n=(l-1)L}^{lL-1} \times \left[\sum_{m \neq n} c_n c_m R_h\left[\left(\hat{\tau}(l) + \left(n \pm \frac{1}{2}\right)T_c\right) - mT_c - \tau_0\right] \cdot \cos(w_\Delta n T_c + \theta_l)\right] + \frac{1}{L} \sum_{n=(l-1)L}^{lL-1} c_n \eta_c\left(n \pm \frac{1}{2}, l\right) \quad (13)$$

$$N_s^{\pm}(l) = \frac{\sqrt{E_c}}{L} \sum_{n=(l-1)L}^{lL-1} \times \left[\sum_{m \neq n} c_n c_m R_h\left[\left(\hat{\tau}(l) + \left(n \pm \frac{1}{2}\right)T_c\right) - mT_c - \tau_0\right] \cdot \sin(w_\Delta n T_c + \theta_l)\right] + \frac{1}{L} \sum_{n=(l-1)L}^{lL-1} c_n \eta_s\left(n \pm \frac{1}{2}, l\right) \quad (14)$$

and $\mathrm{E}[\cdot]$ denotes the expectation operation. The first term in (13) and (14) is the code-self noise and can be neglected for a moderate to large $L$, although it can also be incorporated in the analysis as in [14], [17]. As a result, $\{N_c^{\pm}(l)\}$ and $\{N_s^{\pm}(l)\}$ are independently and identically distributed (i.i.d.) Gaussian variables with zero mean and variance $\sigma^2 = N_0/(2L)$.

From Fig. 1, the error signal $e(l)$ is given by

$$e(l) = \left|\boldsymbol{z}^{+}(l)\right|^2 - \left|\boldsymbol{z}^{-}(l)\right|^2. \quad (15)$$

Again, writing the error signal into the sum of DC and noise terms, (15) becomes

$$e(l) = S(\varepsilon_l) + N_T(l) \quad (16)$$

where

$$S(\varepsilon_l) \doteq \mathrm{E}[e(l)] = \mathrm{E}^2\left[z_c^+(l)\right] + \mathrm{E}^2\left[z_s^+(l)\right] - \mathrm{E}^2\left[z_c^-(l)\right] - \mathrm{E}^2\left[z_s^-(l)\right] \tag{17}$$

is the actually the $S$-curve of the loop, the useful term for tracking the code phase $\tau(t)$ through the quantizer, loop filter, and numerical control oscillator (NCO). The total noise $N_T(l)$ is defined as

$$N_T(l) = N_1(l) + N_2(l) \tag{18}$$

where

$$N_1(l) = \left(N_c(l)^+\right)^2 + \left(N_s(l)^+\right)^2 - \left(N_c(l)^-\right)^2 - \left(N_s(l)^-\right)^2 \tag{19}$$

and

$$N_2(l) = 2\left\{\mathrm{E}\left[z_c^+(l)\right] N_c^+(l) + \mathrm{E}\left[z_s^+(l)\right] N_s^+(l) - \mathrm{E}\left[z_c^-(l)\right] N_c^-(l) - \mathrm{E}\left[z_s^-(l)\right] N_s^-(l)\right\}. \tag{20}$$

Clearly, $\{N_T(l)\}$ are non-Gaussian i.i.d. random variables, although they have been approximated as Gaussian in previous analysis [14]–[16].

For $aL \ll 1$, the case of practical interest, then $\tau(lL) \approx \tau(lL+i)$, $i = 0 \cdots L-1$, and hence, (11) and (12) become

$$E\left[z_c^{\pm}(l)\right] \approx \frac{\sqrt{E_c}}{L} R_h\left(\left(\varepsilon_l \mp \frac{1}{2}\right) T_c\right) \times \sum_{n=(l-1)L}^{lL-1} \cos(w_\Delta n T_c + \theta_l) \tag{21}$$

and

$$E\left[z_s^{\pm}(l)\right] \approx \frac{\sqrt{E_c}}{L} R_h\left(\left(\varepsilon_l \mp \frac{1}{2}\right) T_c\right) \times \sum_{n=(l-1)L}^{lL-1} \sin(w_\Delta n T_c + \theta_l) \tag{22}$$

where $\varepsilon_l = [\tau(lL) - \hat{\tau}(l)]/T_c$, is the normalized tracking error at the instant of $l \cdot LT_c$, and

$$S(\varepsilon_l) \approx E_c D^2(w_\Delta)\left[R_h^2\left(\left(\varepsilon_l - \frac{1}{2}\right) T_c\right) - R_h^2\left(\left(\varepsilon_l + \frac{1}{2}\right) T_c\right)\right] \tag{23}$$

with

$$D(w_\Delta) = \frac{1}{L} \cdot \sin\left(\frac{L w_\Delta T_c}{2}\right) \mathrm{cosec}\left(\frac{w_\Delta T_c}{2}\right). \tag{24}$$

In (23), $R_h^2((\varepsilon_l - 1/2)T_c) - R_h^2((\varepsilon_l + 1/2)T_c)$ is the $S$-curve of the noncoherent DLL with no Doppler shift, and $D^2(w_\Delta)$ is the well-known SNR loss due to the carrier frequency discrepancy $w_\Delta$.

As is mentioned, in digital DLLs, the adaptation of code tracking can only be done in discrete steps. In Fig. 1, the quantizer $Q_\delta(e)$ which quantizes the error signal $e(l)$ is employed to investigate this effect. The quantizer has the following input and output characteristics:

$$e^* \doteq Q_\delta(e) = \begin{cases} \alpha & e > \left(q - \frac{1}{2}\right)\delta \\ k \cdot \frac{\alpha}{q} & \left(k - \frac{1}{2}\right)\delta < e \le \left(k + \frac{1}{2}\right)\delta; \\ -\alpha & e < -\left(q - \frac{1}{2}\right)\delta, \\ & -(q-1) \le k \le q-1 \end{cases} \tag{25}$$

where $\alpha$ is the quantization limit, $\delta \doteq \alpha/q$ is the unit quantization level and $2q+1$ is the total number of quantization levels.

In addition, since we consider the second-order loop, $F(z)$, the transfer function of the loop filter, is given by $F(z) = g_1 + g_2/(1 - z^{-1})$, where $g_1$ and $g_2$ are constants, and, as usual, NCO is modeled as $D(z) = z^{-1}/(1 - z^{-1})$. If $g_2 = 0$, the loop becomes a first order. By using (15) and Fig. 1, the nonlinear model for the digital DLL is obtained as in Fig. 2.

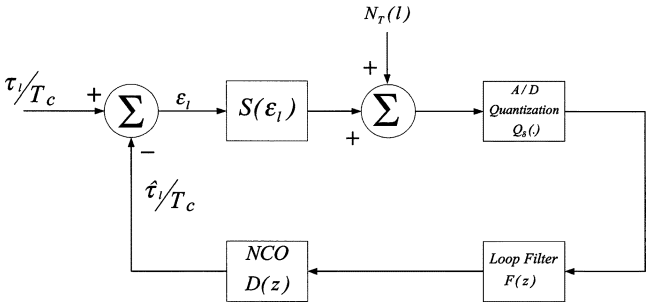


Fig. 2. Nonlinear baseband equivalent model for digital DLL.

## III. Performance Analysis

As discussed, for GPS and/or other satellite based broadcasting DSSS systems, PN code synchronization follows a procedure of combined tracking/reacquisition/trackin, etc., after an initial acquisition. That is, during tracking whenever $|\varepsilon_l| > \varepsilon_{max} > 0$, a new acquisition will be initiated and a new tracking follows. Hence, for a stationary channel as we considered here, the tracking process will restart itself after each code reacquisition and, hence, can be modeled as a regenerative process [20]. In the following, the independent tracking process after each reacquisition will be named as an element process of the regenerative process, and MTLL and MSE will be analyzed based on this regenerative process modeling of the tracking process.

Starting from Fig. 2 and following a procedure similar to that in [17], [21], it can be shown that for an element process of the regenerative tracking process

$$\varepsilon_1 = a \cdot L + \varepsilon_0 - (g_1 + g_2) Q_\delta\left[S(\varepsilon_0) + N_T(0)\right] \tag{26}$$

and for $l \ge 1$

$$\varepsilon_{l+1} - 2\varepsilon_l + \varepsilon_{l-1} = -(g_1 + g_2) Q_\delta\left[S(\varepsilon_l) + N_T(l)\right] + g_1 Q_\delta\left[S(\varepsilon_{l-1}) + N_T(l-1)\right]. \tag{27}$$

Define

$$\gamma \doteq 1 + \frac{g_2}{g_1} \tag{28}$$

and

$$\varepsilon_l \doteq u_l - \gamma u_{l+1}, \quad l \ge 0. \tag{29}$$

Then, from (27), we have

$$u_{l+1}=2u_l-u_{l-1}+g_1Q_\delta\left[S(u_{l-1}-\gamma u_l)+N_T(l-1)\right],\ \ l\geq 2 \tag{30}$$

with the initial conditions $u_0$, $u_1$, and $u_2$ determined by

$$\varepsilon_0=u_0-\gamma u_1 \tag{31}$$

and

$$\varepsilon_1=u_1-\gamma u_2. \tag{32}$$

Furthermore, let $y_1(l)\doteq u_l$ and $y_2(l)\doteq u_{l+1}$, the element tracking process can be described by the following state equations:

$$y_1(l)=y_2(l-1) \tag{33}$$

and

$$y_2(l)=2y_2(l-1)-y_1(l-1)+g_1Q_\delta \times\left[S\left(y_1(l-1)-\gamma y_2(l-1)\right)+N_T(l-1)\right]. \tag{34}$$

Since $\{N_T(l)\}$ are stationary white noises, it is evident that (33) and (34) describe a homogeneous two-dimensional Markov chain.

Define $\Delta\doteq g_1/I\cdot\alpha/q$, where $I$ is a positive integer, and let $\varepsilon_0$ and $\varepsilon_1$ be quantized to the values of $i\Delta$ and $j\Delta$, respectively. Then, from (30)–(34), $u_l$ and, hence, $y_1(l)$ and $y_2(l)$, will take on the values of multiples of $\Delta$, if $\gamma$ is a rational number[1] and $u_0$, $u_1$, and $u_2$ in (31) and (32) are properly selected. Note that from (34), $I\Delta$ is the unit adaptation step of the loop and $\Delta$ is a parameter relevant to the resolution of analysis. For example, from (29), the tracking error $\varepsilon$ can only take the values of multiple $\Delta$, if $\gamma$ is a positive integer. ($\gamma=2$ has been known to give the best transient response for the case with no quantization [17], [21].)

### A. Mean Time-to-Lose Lock

Define $\mathcal{N}$ be the number of steps from the start of an (element) Markov chain to reach the absorbing state. The absorbing state is the state with $|\varepsilon_l=y_1(l)-\gamma y_2(l)|>\varepsilon_{max}$. By definition, the MTLL of an element process is given by

$$\begin{aligned}\mathrm{MTLL}&=\sum_{l=1}^{\infty}lP_r\{\mathcal{N}=l\}\\&=\sum_{l=1}^{\infty}l\left(P_r\{\mathcal{N}\geq l\}-P_r\{\mathcal{N}>l\}\right).\end{aligned} \tag{35}$$

Since $P_r\{\mathcal{N}\geq l\}$ is the probability that the loop still remains in lock at the $l-1$ step, i.e.,

$$P_r\{\mathcal{N}\geq l\}=\sum_{\varepsilon(m)\in\mathcal{M}}P_{\varepsilon_{l-1}}\left(\varepsilon(m)\right) \tag{36}$$

where $P_{\varepsilon_l}(\varepsilon(m))=P_r\{\varepsilon_l=\varepsilon(m)\}$ and $\mathcal{M}$ is the set of possible $|\varepsilon|\leq\varepsilon_{max}$ defined in (29), (35) can be rewritten as

$$\begin{aligned}\mathrm{MTLL}&=1+\sum_{\varepsilon(m)\in\mathcal{M}}\sum_{l=1}^{\infty}P_{\varepsilon_l}\left(\varepsilon(m)\right)\\&=1+\sum_{\varepsilon(m)\in\mathcal{M}}T\left(\varepsilon(m)\right)\end{aligned} \tag{37}$$

where $T(\varepsilon(m))=\sum_{l=1}^{\infty}P_{\varepsilon_l}(\varepsilon(m))$. Furthermore, define $P_{\boldsymbol{y}(l)}(i,j)=P_r\{y_1(l)=i\Delta,y_2(l)=j\Delta\}$ and $T_{\boldsymbol{y}}(i,j)=\sum_{l=1}^{\infty}P_{\boldsymbol{y}(l)}(i,j)$, then from (29), (33), and (34), we also have

$$\mathrm{MTLL}=1+\sum_{i=-K}^{K}\sum_{j=-K}^{K}T_{\boldsymbol{y}}(i,j). \tag{38}$$

In Appendix A, it is shown that for $|\varepsilon_l|\leq\varepsilon_{max}$, $-K\Delta\leq y_1$, $y_2\leq K\Delta$ for some positive integer $K$. In addition, $T_{\boldsymbol{y}}(i,j)=0$ for some of the states in the set $\{\boldsymbol{y}=(y_1,y_2)|-K\Delta\leq y_1(l),y_2(l)\leq K\Delta\}$, i.e., not all the states are legitimate states. (The legitimate states are actually the transient states of the (element) Markov chain.) For simplicity of notation, however, the illegitimate states are also included in (38). The same practice will be employed in (39)–(45).

According to the homogeneous Markovian property, it can be shown that

$$\begin{aligned}T_{\boldsymbol{y}}(i,j)=&\sum_{n=-K}^{K}P_{\boldsymbol{y}|\boldsymbol{y}}(i,j|n,i)T_{\boldsymbol{y}}(n,i)\\&+\sum_{n=-K}^{K}P_{\boldsymbol{y}|\boldsymbol{y}}(i,j|n,i)P_{\boldsymbol{y}(1)}(n,i)\end{aligned} \tag{39}$$

where $P_{\boldsymbol{y}|\boldsymbol{y}}(i,j|r,s)$ is the transition probability from the state $(y_1(l-1)=r\Delta,\ y_2(l-1)=s\Delta)$ to the state $(y_1(l)=i\Delta,\ y_2(l)=j\Delta)$. Since $y_1(l)=y_2(l-1)$, $P_{\boldsymbol{y}|\boldsymbol{y}}(i,j|r,s)=0$, if $i\neq s$. (39) can also be written in matrix form as follows:

$$\boldsymbol{T}=\boldsymbol{b}+\boldsymbol{Q}\boldsymbol{T} \tag{40}$$

and

$$(\boldsymbol{I}-\boldsymbol{Q})\boldsymbol{T}=\boldsymbol{b} \tag{41}$$

where

$$\begin{aligned}\boldsymbol{T}=&[T_{\boldsymbol{y}}(-K,-K)\cdots T_{\boldsymbol{y}}(-K,K)\cdots\\&\cdots T_{\boldsymbol{y}}(K,-K)\cdots T_{\boldsymbol{y}}(K,K)]^T\end{aligned} \tag{42}$$

$$\begin{aligned}\boldsymbol{b}=&[b(-K,-K)\cdots b(-K,K)\cdots\\&\cdots b(K,-K)\cdots b(K,K)]^T\end{aligned} \tag{43}$$

$$b(i,j)=\sum_{n=-K}^{K}P_{\boldsymbol{y}|\boldsymbol{y}}(i,j|n,i)P_{\boldsymbol{y}(1)}(n,i) \tag{44}$$

and (45), located at the bottom of the page. Thus, the problem of finding MTLL reduces to solving the system of linear equations in (41). Before to proceed further, three observations are in order. First, the equations associated with $T_{\boldsymbol{y}}(i,j)=0$ in (41)

[1]This will practically place no restriction on the applicability of this method.

should be removed, i.e., $(y_1(l) = i\Delta, y_2(l) = j\Delta)$ is an unallowed state. Second, $\boldsymbol{Q}$ is a sparse matrix and, after removing the rows and columns corresponding to the illegitimate states, is actually the transition matrix for the transient states of the Markov chain. Third, the system of linear equations (41) might have a very large dimension, depending the numbers $q$ and $\Delta$. As an example, $\boldsymbol{T}$ is a 2113 $\times$ 2113 matrix for the numerical examples in Section IV. Hence, the direct solution methods such as Gaussian elimination or matrix factorization may be too complex to be used. On the other hand, however, since $\boldsymbol{Q}$ is a sparse matrix, iterative methods is expected to provide a solution more efficiently [22].

From (34), the transition probability $P_{\boldsymbol{y}|\boldsymbol{y}}(i,j|r,i)$ is given by

$$P_{\boldsymbol{y}|\boldsymbol{y}}(i,j|r,i) = P_r\left\{g_1 Q_\delta\left[S\left((r-\gamma i)\Delta\right) + N_T(l-1)\right] = (j-2i+r)\Delta\right\} \quad (46)$$

or equivalently, $P_{\boldsymbol{y}|\boldsymbol{y}}(i,j|r,i) = P_r\{N_T(l) < -(q-1/2)\delta - S(r\Delta - \gamma i\Delta)\}$ for $j-2i+r=-q$, $P_{\boldsymbol{y}|\boldsymbol{y}}(i,j|r,i) = P_r\{(j-2i+r-1/2)\delta - S((r-\gamma i)\Delta) \le N_T(l) \le (j-2i+r+1/2)\delta - S((r-\gamma i)\Delta)\}$ for $j-2i+r = -(q-1)\cdots(q-1)$, and $P_{\boldsymbol{y}|\boldsymbol{y}}(i,j|r,i) = P_r\{N_T(l) > (q-1/2)\delta - S((r-\gamma i)\Delta)\}$ for $j-2i+r = q$. Clearly, the transition probability can be evaluated if the cumulative probability density (CDF) or complementary CDF of the random variable $N_T(l)$ is known. In Appendix B, the method of saddle point integration is employed to evaluate complementary CDF of $N_T(l)$. This evaluation is more accurate than the previous analysis, where $N_T(l)$ is assumed to be a Gaussian variable.

Let $\boldsymbol{A} = \boldsymbol{I} - \boldsymbol{Q}$, (41) becomes

$$\boldsymbol{A}\boldsymbol{T} = \boldsymbol{b} \quad (47)$$

where the equations associated with $T_{\boldsymbol{y}}(i,j) = 0$ in (41) have been removed implicitly. In Appendix B, it is shown that $\boldsymbol{A}$ is an $M$-matrix and, hence, the iterative successive relaxation method (SOR) can be used to solve (47) in a way that is much more efficient than the direct solution method [22]. As in [22], let

$$\boldsymbol{A} = \boldsymbol{D} - \boldsymbol{L} - \boldsymbol{U} \quad (48)$$

where $\boldsymbol{D}$ is the diagonal matrix consisting of the main diagonal elements of $\boldsymbol{A}$, and $\boldsymbol{L}$ and $\boldsymbol{U}$ are the lower and upper block matrix triangular parts of $\boldsymbol{A}$, respectively. Then, the SOR iterative algorithm is given by

$$(\boldsymbol{D} - w\boldsymbol{L})\boldsymbol{T}^{i+1} = [(1-w)\boldsymbol{D} + w\boldsymbol{U}]\boldsymbol{T}^i + w\boldsymbol{b}, \qquad i = 0, 1\cdots \quad (49)$$

where $\boldsymbol{T}^i$ is the approximate solution at the stage $i$, and $w$ is the algorithm parameter, called relaxation parameter that needs to be determined for the fastest convergent rate.

### B. MSE

As discussed, the operation of code tracking can be modeled as a regenerative Markov chain. Hence, from Theorem 3.7.1 of [20], the stationary state probability at the state $\varepsilon = \varepsilon(m)$ (of the regenerative Markov chain) is given by (50),[2] located at bottom of the following page. In (50), $T(\varepsilon(m))$ can be evaluated by using (29), after $T_{\boldsymbol{y}}(i,j)$ is solved in (47). Hence, the MSE can be evaluated easily as follows:

$$\mathrm{MSE} = \sum_{\varepsilon(m)\in\mathcal{M}} P\left(\varepsilon(m)\right)\cdot\varepsilon^2(m). \quad (51)$$

## IV. Numerical Results

For the numerical results that follow, the following set of system parameters are employed: $\varepsilon_{max} = 0.5$, $L = 128$, $\Delta = 1/64$, $w_\Delta = 0$, and $h(t) = 1/\sqrt{T_c}$, $0 \le t \le T_c$ and $h(t) = 0$, otherwise. Here, $\Delta = 1/64$ means that the analysis resolution is $1/64 \cdot T_c$. Basically, the selection of $g_1$ and $\gamma$ is a tradeoff between the tracking error due to noise and the ability to track the dynamics of the input code phase. Here, we are mainly concerned with the effect of discrete adaptation, and hence the fixed values of $g_1 = 1/(4E_c)$ and $\gamma = 2$ are used throughout.

Two extreme cases will be employed to examine the effects of discrete adaptation on the loop behaviors, including the transient response, lock-in range, MSE and MTLL. The first (Case I) is to fix the quantization limit $\alpha$ to $E_c$, the maximum value of $S$-curve, and $q$ (hence, $I$) is varied to see the effects. Recall that $\Delta = g_1/I\cdot\alpha/q$, and $I\Delta$ is the unit adaptation step. The other (Case II) is to fix $I\Delta$ equal to 1/64, i.e., $I = 1$, and $\alpha$ is then changed according to $\alpha = q\cdot E_c/16$. In practice, however, the selection $\alpha$ and $q$ is often a tradeoff between performance and complexity.

Figs. 3 and 4 show example effects of quantized adaptation on the transient response of the loop. For Case I, $q \ge 16$ behaves almost the same as the continuous adaptation (no quantization) case. However, a large tracking error is observed for $q \le 4$ due to large quantization error. On the other hand, for Case II, the convergence of the loop is slowed significantly for $q \le 2$ because of the limitation on the value of $\alpha$. That is the useful signal for error correction has been cut off. The tracking error is not much different for different $q$ after convergence, though. In Figs. 3 and 4, the residual tracking error for the case of no quantization is due to the distortion in $S$-curve incurred by a large code Doppler shift [5].

[2]Note that for an element process, $P(\varepsilon(m)) = 0\ \forall\ m$ because eventually the process will lose lock.

$$\boldsymbol{Q} = \begin{bmatrix} P_{\boldsymbol{y}|\boldsymbol{y}}(-K,-K|-K,-K)0\cdots0 & \cdots\cdots & P_{\boldsymbol{y}|\boldsymbol{y}}(-K,-K|K,-K)0\cdots0 \\ \vdots & \vdots & \vdots \\ P_{\boldsymbol{y}|\boldsymbol{y}}(-K,-K|-K,-K+1)0\cdots0 & \cdots\cdots & P_{\boldsymbol{y}|\boldsymbol{y}}(-K,-K|K,-K+1)0\cdots0 \\ \vdots & \vdots & \vdots \\ \vdots & \vdots & \vdots \\ \vdots & \vdots & \vdots \\ P_{\boldsymbol{y}|\boldsymbol{y}}(-K,-K|-K,K)0\cdots0 & \cdots\cdots & P_{\boldsymbol{y}|\boldsymbol{y}}(-K,-K|K,K)0\cdots0 \end{bmatrix} \quad (45)$$

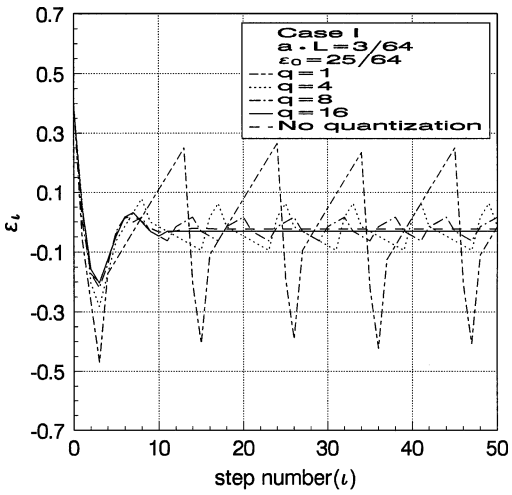


Fig. 3. Effects of quantized adaptation on the transient response.

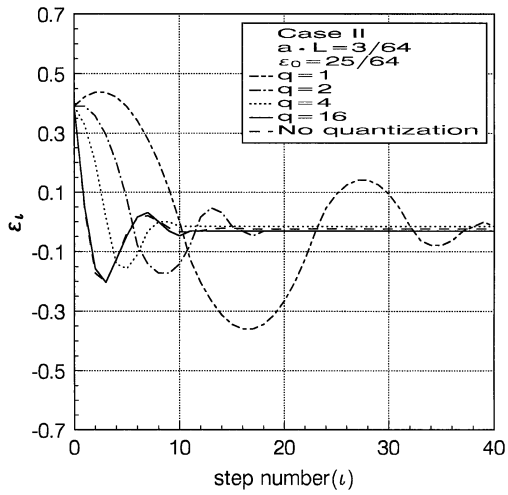


Fig. 4. Effects of quantized adaptation on the transient response.

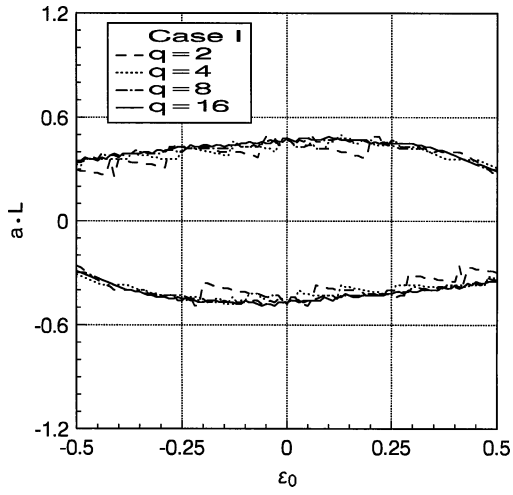


Fig. 5. Effects of quantized adaptation on the lock-in range.

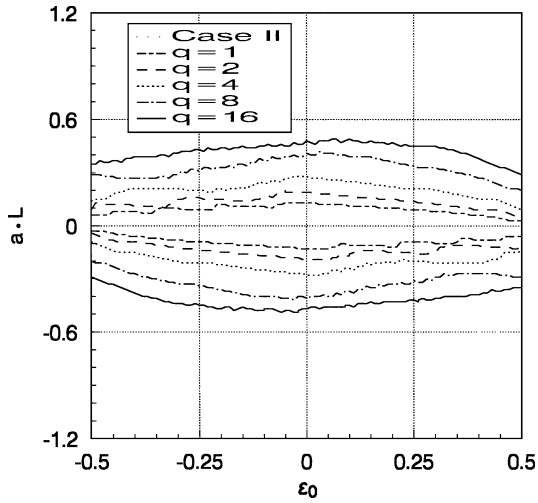


Fig. 6. Effects of quantized adaptation on the lock-in range.

Figs. 5 and 6 are the loop lock-in ranges with different quantization levels. The lock-in rage is defined as the range of initial conditions $[aL, \varepsilon_0]$ such that the tracking error will never exceed $\varepsilon_{\max}$ during the subsequent tracking process, i.e., no reacquisition. For case I, the lock-in range varies slightly for $q \geq 2$. (For $q = 1$, the lock-in range is very irregular because of very large quantization error.) For Case II, on the other hand, the lock-in range is significantly reduced for a small $q$, again because of the incurred limitation on the value of $\alpha$. Note that the lock-in range is odd-symmetric with respect to $\varepsilon_0 = 0$ because of the very same property associated with the $S$-curve [5].

Fig. 7 shows the effects of quantized adaptation on MSE and MTLL for case I. As is evident, for a large code Doppler, too small a $q$ will result in a significant performance loss; $q \geq 4$ is a necessity in this case. Fig. 8 shows the same effects for Case II. As seen, unlike Case I an optimal $q$ exists, depending on SNR; a large $q$ not necessarily gives a better performance. This is especially true at low SNRs, where the tail ends of $N_T(l)$ impose a significant adverse effect on the loop performance.

$$
\begin{aligned}
P(\varepsilon(m)) &\doteq \lim_{l\to\infty} P_r\{\varepsilon_l = \varepsilon(m)\} \\
&= \frac{\mathrm{E}[\text{amount of time in state } \varepsilon = \varepsilon(m) \text{ during an element process}]}{MTLL} \\
&= \frac{\sum_{l=1}^{\infty} 1 \cdot P_{\varepsilon_l}(\varepsilon(m))}{MTLL} \\
&= \frac{T(\varepsilon(m))}{MTLL}
\end{aligned}
\tag{50}
$$

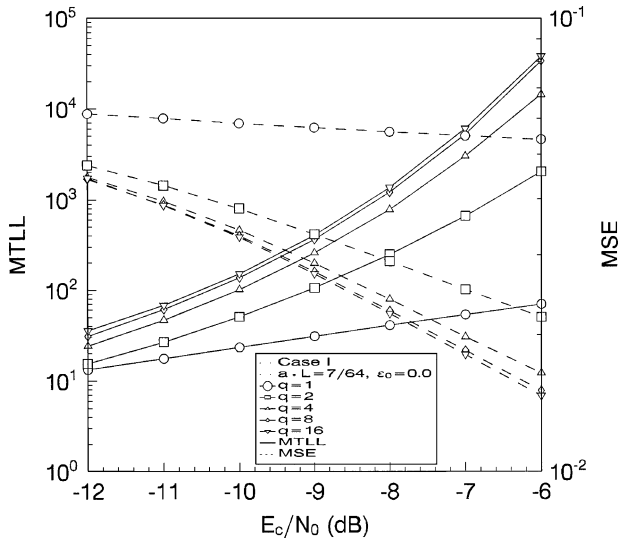


Fig. 7. Effects of quantized adaptation on MSE and MTLL.

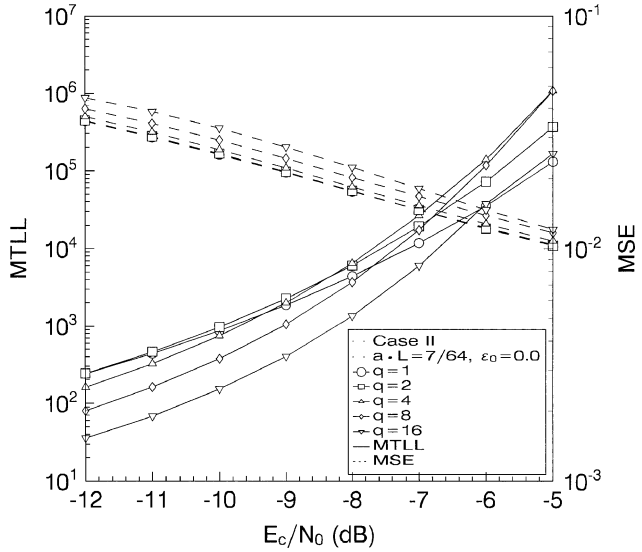


Fig. 8. Effects of quantized adaptation on MSE and MTLL.

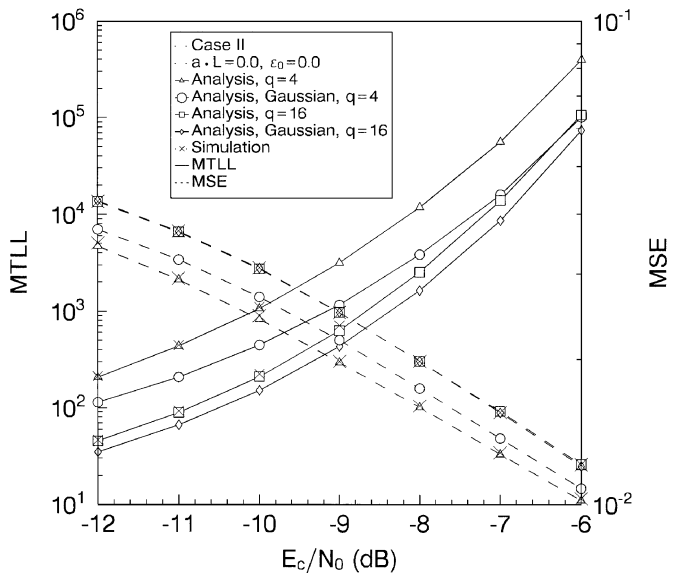


Fig. 9. Comparisons of MSE and MTLL with those obtained with Gaussian approximation.

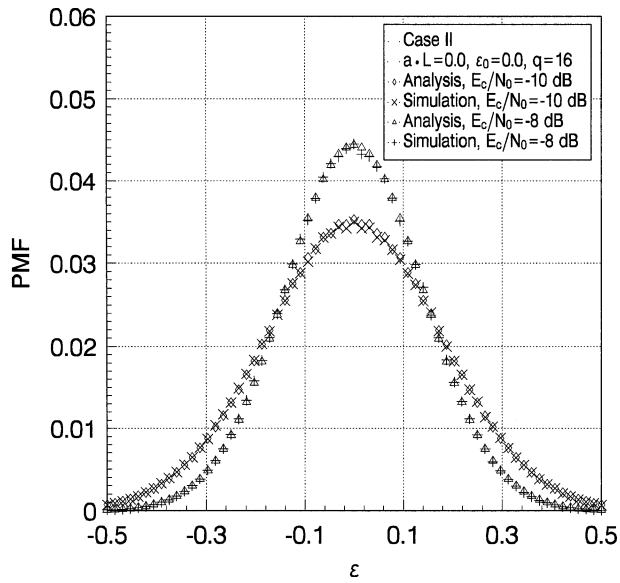


Fig. 10. Example probability mass functions.

Fig. 9 compares the MSE and MTLL with those obtained by using Gaussian approximation for Case II. It is clear in the figure that the analysis based on the Gaussian approximation may result in a large error for a small $q$. Nevertheless, it becomes more accurate for a large $q$, as already discussed in previous analysis where quantization is not taken into account [14]–[16]. Fig. 9, simulation results are also given and that agree very well with the analysis. The simulations are Fig. 11 gives example probability mass functions. Again, the simulations agree very well with the analysis.

## V. Conclusion

The noncoherent second-order digital delay lock loops for direct sequence spread spectrum systems is analyzed with the presence of Doppler shift. A new analysis based on a regenerative Markov chain modeling of the tracking process is proposed with the loop quantized adaptation being taken into account that has been neglected in previous analysis. For second order loops, it is shown that the transition matrix of the transient states of the Markov chain is a sparse matrix with a very nice property, called $M$-matrix, that leads to an efficient analysis. Numerical results show that quantized adaptation has a significant impact on the loop performance, including transient responses, lock-in range, MSE, and MTLL. In addition, without imposing a Gaussian approximation in the analysis, MTLL and MSE are evaluated more accurately than previous methods.

## Appendix A

In this Appendix, we discuss the range of $y_1(l)$ and $y_2(l)$ for the tracking loop to remain in lock. From (34), it can be shown that

$$y_2(l)+(\gamma-2)y_1(l) = -\varepsilon_{l-1} + g_1 Q_\delta \times \left[S\left(y_1(l-1)-\gamma y_2(l-1)\right)+N_T(l-1)\right]. \quad \text{(A-1)}$$

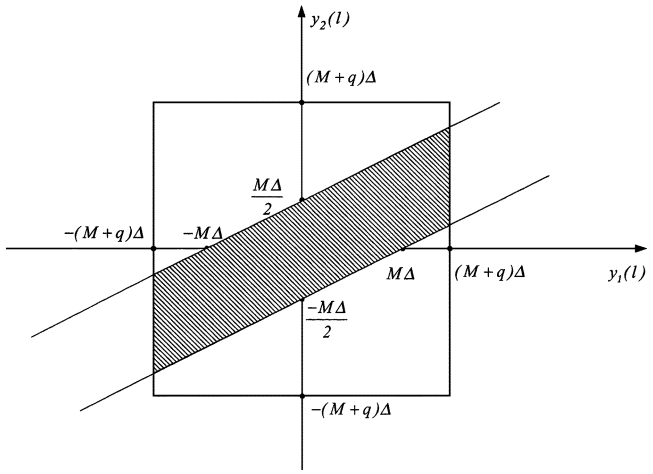


Fig. 11. Range of $y_1(l)$ and $y_2(l)$ for $I = 1$ and $\gamma = 2$.

Since $|g_1 Q_\delta[\cdot]| \leq qI\Delta$, we have

$$|y_2(l) + (\gamma - 2)y_1(l)| \leq (M + qI)\Delta \tag{A-2}$$

where $M = \lfloor \varepsilon_{max}/\Delta \rfloor$, $\lfloor x \rfloor$ is the largest integer less than $x$, and $|\varepsilon_l| \leq M\Delta$ for the tracking loop to remain in lock. On the other hand, since $\varepsilon_l = y_1(l) - \gamma y_2(l)$, we also have

$$|y_1(l) - \gamma y_2(l)| \leq M\Delta. \tag{A-3}$$

Finally, by definition

$$y_1(l) = y_2(l-1) \tag{A-4}$$

and, hence, $y_1(l)$ and $y_2(l)$ has the same range. From (A-2)–(A-4), it is clear that $-K\Delta \leq y_1(l), y_2(l) \leq K\Delta$ for some positive integer $K < \infty$. As an example, Fig. 11 shows the range of $y_1(l)$ and $y_2(l)$ for the cases of $\gamma = 2$ and $I = 1$, where $K = M + q$. In addition, from Fig. 11, we note that not all the states $\boldsymbol{y} = (y_1(l), y_2(l))$ within the range of $-K\Delta \leq y_1(l), y_2(l) \leq K\Delta$ are legitimate states, due to the constraint in (A-2)–(A-4), where $i = j = K$ for $\gamma = 2$ is one of such examples.

## Appendix B

In this Appendix, the saddle-point integration is used for calculating the probability of

$$P_{N_T}(x) \triangleq \int_x^\infty f_{N_T}(n_t) dn_t, \quad x \geq 0 \tag{B-1}$$

where $f_{N_T}(n_t)$ is the probability density function (pdf) of $N_T(l)$. Recall that $\{N_T(l)\}$ are i.i.d. random variables. Let $\Psi_{N_T}(s)$ be the moment generating function of $N_T$. That is

$$\begin{aligned}\Psi_{N_T}(s) &\triangleq \mathrm{E}[e^{-sN_T}] \\ &= \int_{-\infty}^{\infty} e^{-sn_t} f_{N_t}(n_t) dn_t.\end{aligned} \tag{B-2}$$

Then, (B-1) becomes

$$P_{N_T}(x) = \frac{1}{2\pi \boldsymbol{j}} \int_{c-\boldsymbol{j}\infty}^{c+\boldsymbol{j}\infty} \frac{\Psi_{N_T}(s)}{-s} \cdot \exp[sx]\, ds \tag{B-3}$$

where $s = c + \boldsymbol{j}z$ with $c < 0$. For easy of computation, we define

$$\Phi_{N_T}(s) = \log\left[\frac{\Psi_{N_T}(s)}{s} \cdot \exp[sx]\right]. \tag{B-4}$$

Then

$$\begin{aligned}P_{N_T}(x) &= \frac{-1}{2\pi \boldsymbol{j}} \int_{c-\boldsymbol{j}\infty}^{c+\boldsymbol{j}\infty} \exp\left[\Phi_{N_T}(s)\right] ds \\ &= \frac{-1}{\pi} \int_0^\infty \mathrm{Re}\left\{\exp\left[\Phi_{N_T}(c + \boldsymbol{j}z)\right]\right\} dz.\end{aligned} \tag{B-5}$$

In (B-5), we have used the property that $\mathrm{Re}\{\exp[\Phi(c_o + \boldsymbol{j}z)]\}$ is an even function of $z$ [23]. The integration (B-5) would be most efficient if carried along the path of steepest descent of the integrand. For simplicity, however, the integration path is usually deformed to a straight line that passes through the saddle point of the integrand [23]. This method of integration is the so called saddle-point integration. The saddle point $c_o$ is the negative root of the equation

$$\Phi'_{N_T}(c) = 0 \tag{B-6}$$

where $\Phi'_{N_T}(c)$ is the first derivative of $\Phi(c)$. Since for $c < 0$, $\exp[\Phi(c)]$ is a convex function, there is only one negative root in the (B-6) [23]. After obtaining the saddle point, then the integration (B-5) can be evaluated by using the trapezoidal rule as follows [23].

$$P_{N_T}(x) \approx \frac{-dz}{\pi} \cdot \mathrm{Re}\left[\frac{1}{2}\exp[\Phi(c_o)] + \sum_{l=1}^{\mathcal{L}} \exp[\Phi_{N_T}(c_o + \boldsymbol{j}ldz)]\right] \tag{B-7}$$

for a positive integer $\mathcal{L}$. The approximation (B-7) can be made as accurate as desired by using a large and a small enough $\mathcal{L}$ and $dz$, respectively. As in [23], the step size $dz$ can be initially taken as

$$dz = \left[\Phi''_{N_T}(c_o)\right]^{-\frac{1}{2}} \tag{B-8}$$

and then halved successively until the desired precision is obtained.

From (18)–(20), $N_T(l)$ can be written as the following quadratic form:

$$N_T(l) = \boldsymbol{t}^T \boldsymbol{W} \boldsymbol{t} + \boldsymbol{c}^T \boldsymbol{t} \tag{B-9}$$

where $\boldsymbol{t} = [N_c^+(l) N_s^+(l) N_c^-(l) N_s^-(l)]^T$

$$\boldsymbol{W} = \begin{bmatrix} 1 & 0 & 0 & 0 \\ 0 & 1 & 0 & 0 \\ 0 & 0 & -1 & 0 \\ 0 & 0 & 0 & -1 \end{bmatrix} \tag{B-10}$$

and $\boldsymbol{c} = [c_1\ c_2\ c_3\ c_4]^T$ with $c_1 = 2\mathrm{E}[z_c^+(l)]$, $c_2 = 2\mathrm{E}[z_s^+(l)]$, $c_3 = 2\mathrm{E}[z_c^-(l)]$, and $c_4 = 2\mathrm{E}[z_c^-(l)]$. Note that $\mathrm{E}[\boldsymbol{t}] = \boldsymbol{0}$, and

$$\boldsymbol{V} \doteq \mathrm{E}[\boldsymbol{t}\boldsymbol{t}^T] = \begin{bmatrix} \sigma^2 & 0 & 0 & 0 \\ 0 & \sigma^2 & 0 & 0 \\ 0 & 0 & \sigma^2 & 0 \\ 0 & 0 & 0 & \sigma^2 \end{bmatrix}. \tag{B-11}$$

From [24], the moment generating function for this quadratic form is given by

$$\Psi_{N_T}(s) = |\boldsymbol{I}+2s\boldsymbol{W}\boldsymbol{V}|^{-\frac{1}{2}} \exp\left\{\frac{s^2}{2}\cdot \boldsymbol{c}^T\boldsymbol{V}(\boldsymbol{I}+2s\boldsymbol{W}\boldsymbol{V})^{-1}\boldsymbol{c}\right\}. \tag{B-12}$$

With this $\Psi_{N_T}(s)$, the probability (B-1) can be evaluated by using (B-7).

## APPENDIX C

In this Appendix, we prove that $\boldsymbol{A}$ in (47) is an $M$-matrix, so that the successive over relaxation (SOR) iterative method is convergent and can be employed to solve (47) very efficiently. Before to proceed, the following definitions and theorem are useful.

*Definition 1 [22]:* A matrix $\boldsymbol{X} = [x_{ij}]$ is said to be nonnegative, denoted $\boldsymbol{X} \geq 0$, if $x_{i,j} \geq 0$.

*Definition 2 [22]:* A real-square matrix $\boldsymbol{X} = [x_{ij}]$ is called a nonsingular $M$-matrix if $x_{i,j} \leq 0$ for $i \neq j$, and if it is monotone, i.e., $\boldsymbol{X}^{-1} \geq 0$.

*Theorem 1 (Lemma 5.2 in [22]):* For a arbitrary square matrix $\boldsymbol{X} = [x_{ij}]$.

1) $\lim_{k\to\infty} \boldsymbol{X}^k = \boldsymbol{0}$, iff $\rho(\boldsymbol{X}) < 1$, where $\rho(\boldsymbol{X})$, called spectral radius, is the maximum absolute value of any eigenvalues of $\boldsymbol{X}$.
2) If $\rho(\boldsymbol{X}) < 1$, then $(I - \boldsymbol{X})^{-1} = \boldsymbol{I} + \boldsymbol{X} + \boldsymbol{X}^2 + \cdots$ is convergent.

*Theorem 2:* The matrix $\boldsymbol{A} = \boldsymbol{I} - \boldsymbol{Q}$ is an $M$-matrix.

*Proof:* First, since $\boldsymbol{Q}$ is the transition matrix of the transients states of a Markov chain, $\lim_{k\to\infty} \boldsymbol{Q}^k = \boldsymbol{0}$, and $\boldsymbol{A} = [a_{ij}]$, $a_{i,j} \leq 0$, for $i \neq j$. Second, from Theorem 1, $\boldsymbol{A}^{-1} = \boldsymbol{I} + \boldsymbol{Q} + \boldsymbol{Q}^2 + \cdots$ is convergent and $\boldsymbol{A}^{-1} \geq 0$. From the definition 1, the theorem follows.

## REFERENCES


[1] M. K. Simon, J. K. Omura, R. A. Scholtz, and B. K. Levitt, *Spread Spectrum Communications*. Rockville, MD: Computer Science Press, 1985, vol. III.

[2] R. L. Peterson, R. E. Ziemer, and D. E. Borth, *Introduction to Spread Spectrum Communications*. Englewood Cliffs, NJ: Prentice-Hall, 1995.

[3] M. El-Tarhuni and A. Ghrayeb, "A multipath resistant PN code tracking algorithm," in *Proc. IEEE Int. Symp. Personal, Indoor, and Mobile Radio Communications (PIMRC)*, Sept. 2002, pp. 1834–1838.

[4] P. Schulz-Rittich, G. Fock, J. Baltersee, and H. Meyr, "Low-complexity adaptive code tracking with improved multipath resolution for DS-CDMA communication over fading channels," in *Proc. IEEE Int. Symp. Spread Spectrum Techniques Applicat. (ISSSTA)* , Sept. 2000, pp. 30–34.

[5] W.-H. Sheen and C.-H. Tai, "A noncoherent tracking loop with diversity and multipath interference cancellation for direct sequence spread spectrum systems," *IEEE Trans. Commun.*, vol. 46, pp. 1516–1524, Nov. 1998.

[6] W.-H. Sheen and G. L. Stüber, "A new tracking loop for spread-spectrum systems on frequency-selective fading channels," *IEEE Trans. Commun.*, vol. 43, pp. 3063–3072, Dec. 1995.

[7] S. J. Kim and R. A. Iltis, "GPS code tracking with adaptive beamforming and jammer nulling," in *Proc. IEEE 36th Asilomar Conf. Signals, Systems Computers*, Mar. 2000, pp. 118–124.

[8] D. Gustafson, J. Dowdle, and K. Flueckiger, "A deeply integrated adaptive GPS-based navigator with extended rang code tarcking," in *Proc. IEEE Position Location and Navigation*, Nov. 2002, pp. 975–979.

[9] M. C. Laxton and S. L. DeVilbiss, "GPS multipath mitigation during code tracking," in *Proc. IEEE American Control Conf.*, June 1997, pp. 1429–1433.

[10] J. Scheim and B. Z. Bobrovsky, "Computationally efficient discriminator for code tracking loops," *IEEE Trans. Veh. Technol.*, vol. 52, pp. 727–732, May 2003.

[11] M. K. Simon, "Noncoherent pseudonoise code tracking performance of spread spectrum receivers," *IEEE Trans. Commun.*, vol. COM-25, pp. 327–345, Mar. 1977.

[12] A. Polydoros and C. L. Weber, "Analysis and optimization of correlative code-tracking loops in spread-spectrum systems," *IEEE Trans. Commun.*, vol. COM-33, pp. 30–43, Jan. 1985.

[13] J. Caffery Jr. and G. L. Stuber, "Effects of multiple-access interference on the noncoherent delay lock loop," *IEEE Trans. Commun.*, vol. 48, pp. 2109–2119, Dec. 2000.

[14] R. D. Gaudenzi, M. Luise, and R. Viola, "A digital chip timing recovery loop for band-limited direct-sequence spread spectrum signals," *IEEE Trans. Commun.*, vol. 41, pp. 1760–1769, Nov. 1993.

[15] K. Kallaman and G. Davis, "Jitter performance of a baseband sampled code tracking loop," *IEEE Trans. Commun.*, vol. 42, pp. 2919–2925, Nov. 1994.

[16] N.-Y. Yen, S.-L. Su, and S.-C. Hsieh, "Performance analysis of digital delay lock loops in the presence of Doppler shift," *IEEE Trans. Commun.*, vol. 44, pp. 668–673, June 1996.

[17] W. Zhuang and J. Tranquilla, "Modeling and analysis for the GPS pseudorange observable," *IEEE Trans. Aerosp. Electron. Syst.*, vol. 31, pp. 739–751, Apr. 1995.

[18] K. J. Quirk and M. Srinivasan, "Analysis of sampling and quantization effects on the performance of PN code tracking loops," in *Proc. IEEE Int. Communications Conf.*, May 2002, pp. 1480–1484.

[19] M. Katayama, A. Ogawa, and N. Morinaga, "Carrier synchronization under Doppler shift of the nongeosataionary satellite communication systems," in *Proc. IEEE Int. Symp. Information Theory Applicat. (ICCS/ISITA)*, 1992, pp. 466–470.

[20] S. M. Ross, *Stochastic Processes*, 2nd ed. New York: Wiley, 1996.

[21] C. A. Pomalaza-Raez and C. D. McGillem, "Digital phase-locked loop behavior with clock and sampler quantization," *IEEE Trans. Commun.*, vol. COM-33, pp. 753–759, Aug. 1985.

[22] O. Axelsson, *Iterative Solution Methods*. Cambridge, U.K.: Cambridge Univ. Press, 1994, ch. 5,6.

[23] C. W. Helstrom, *Elements of Signal Detection and Estimation*. Englewood Cliffs, NJ: Prentice-Hall, 1995.

[24] J. Omura and T. Kailath, "Some useful probability distributions," Stanford Univ., Stanford, CA, Tech. Rep. 7050-6, Sept. 1965.



**Wern-Ho Sheen** (M'91) received the B.S. degree from the National Taiwan University of Science and Technology, Taipei, Taiwan, R.O.C., in 1982, the M.S. degree from the National Chiao Tung University, Hsinchu, Taiwan, in 1984, and the Ph.D. degree from the Georgia Institute of Technology, Atlanta, in 1991.

From 1993 to 2001, he was with the National Chung Cheng University, Chia Yi, Taiwan, where he held positions as a Professor in the Department of Electrical Engineering and the Managing Director of the Center for Telecommunication Research. Since 2001, he has become a Professor in the Department of Communication Engineering, National Chiao Tung University. His research interests include general areas of communication theory, cellular mobile and personal radio systems, adaptive signal processing for wireless communications, spread spectrum communications, and VLSI design for wireless communications systems.

**Ming-Jou Chang** received the B.S. degree from the National Taiwan University of Science and Technology, Taipei, Taiwan, R.O.C., in 1991, and the M.S.E.E. and Ph.D. degrees from the National Chung Cheng University, Chia-Yi, Taiwan, in 1994 and 2000, respectively.

Since September 2000, he has been with the Computer and Communications Laboratories, Industrial Technology Research Institute, Hsinchu, Taiwan, where he is mainly involved in the projects of wireless communications. His research interests include spread-spectrum communications, mobile communications, VOIP, and network security.

**Cheng-Shong Wu** was born in Taoyuan, Taiwan, R.O.C., in 1961. He received the B.S. and M.S. degrees in electrical engineering from National Taiwan University, Taipei, Taiwan, in 1983 and 1985, and Ph.D. degree in electrical engineering from University of Southern California, Los Angeles, in 1990.

In 1991, he was a Visiting Assistant Professor in the Center for Advanced Computer Studies, University of Southwestern Louisiana, Lafayette. He joined the Department of Electrical Engineering, National Chung-Cheng University, Chia Yi, Taiwan, in fall of 1991, and is currently a Professor there. His research interests include broadband networks, wireless networks, queuing theory, and mathematical programming.